Quantum entanglement between excitons in two-dimensional materials

Gabriel P. Martins, Oleg L. Berman, Godfrey Gumbs, and Yurii E. Lozovik

Phys. Rev. B **106**, 104304 — Published 15 September 2022

DOI: 10.1103/PhysRevB.106.104304

Quantum entanglement between excitons in two-dimensional materials

Gabriel P. Martins[1,2], Oleg L. Berman[1,2], Godfrey Gumbs[2,3] and Yurii E. Lozovik[4,5]
[1] *Physics Department, New York City College of Technology, The City University of New York, Brooklyn, NY 11201, USA*
[2] *The Graduate School and University Center, The City University of New York, New York, NY 10016, USA*
[3] *Department of Physics and Astronomy, Hunter College of The City University of New York City University of New York, New York, NY 10065, USA*
[4] *Institute of Spectroscopy, Russian Academy of Sciences, Troitsk, Moscow, Russia 142190*
[5] *Research University Higher School of Economics, Moscow, Russia 101000*
(Dated: August 30, 2022)

The quantum entanglement between two excitons in two-dimensional materials, embedded in an optical microcavity, was investigated. The energy eigenstates of a Jaynes-Cummings like Hamiltonian for two qubits coupled to a single cavity mode have been calculated. The quantum entanglement between such states was estimated by calculating the concurrence between two qubits in each of these eigenstates. According to the results of our calculations, if the system is allowed to decay only through the emission of cavity photons at low temperatures, there is a maximally entangled eigenstate, protected from decay. We demonstrated that the existence of such a state results in the counter-intuitive conclusion that, for some initial states of the system, the fact that the cavity is leaky can actually lead to an increase in the average concurrence on the timescales of the average photonic lifetime. By briefly analyzing the three-qubit model, we have demonstrated that the probability for the entanglement to be preserved is enhanced when the number of qubits is increased. In addition, we calculated the time evolution of the concurrence between a pair of excitons in a strained graphene monolayer.

PACS numbers: PACs

I. INTRODUCTION

Modern quantum technologies and the prospects for their development are based on the use of quantum two-level (2D) systems as qubits. A number of physical realizations of qubits in systems with discrete spectra have been discussed. These include ultra cold ions and atoms in traps, impurities in diamond, and various types of superconducting qubits. Spatially extended semiconductors and new 2D materials, as well as transition metal dichalcogenides (TMDCs) all have a band structure, However, in the presence of transverse magnetic field, a 2D system has a discrete spectrum consisting of degenerate Landau levels. When electrons pass from filled Landau levels to unfilled excited electron states, then due to the Coulomb attraction between electrons and holes, they form 2D magnetoexcitons, the energy of which depends continuously on the integral of motion in a magnetic field, i.e., the magnetic momentum. This integral of motion is a consequence of the invariance of the system with respect to simultaneous translation and gauge transformation (see Refs. [1, 2]). As a result of the continuous dependence of the magnetoexciton energy on the magnetic pulse, the full spectrum of the system is not discrete, but consists of bands (see Ref. [3]).

Low-dimensional 2D materials have been the subject of an enormous amount of scrutiny within the past few decades [4–6], but, ever since the already historic work where Novoselov, Geim and their collaborators managed to obtain both monolayer and bilayer samples of graphene in 2004 [7], interest in the field has increased substantially by the exciting new physical frontiers it opened. Soon thereafter, a great number of researchers began to investigate the properties of graphene [8–10] as well as other 2D materials that quickly followed. All those studies have been very well summarized in a variety of review papers, of which one of the most well-known was published in 2007 by Katsnelson [11]. Fundamentally new properties of 2D systems are exhibited in pseudomagnetic fields, which arise, in particular, upon deformation of graphene (see Refs. [9, 10, 12, 13]). One of the many interesting properties of 2D materials is that it is the perfect environment for the development of magnetoexcitons [3], the pseudoparticle consisting of the bound states of a negatively charged electron and a positively charged hole. There are two types of excitons that can appear on 2D materials. These are direct excitons, when the electron and the hole are on the same layer, and indirect excitons, when they are on different layers.

An interesting discovery in recent years has been the fact that when mechanical strain is applied to a monolayer of graphene, a pseudo-magnetic field is generated within that sheet [14]. For this system, excitons, formed by an electron and a hole in different valleys, have dispersionless Landau levels [15], whereas excitons in a uniform external magnetic field display a non-trivial energy dispersion relation [3]. This gives rise to well defined energy gaps and might be employed as qubits, if one considers only the ground state and first excited state of each exciton. Our focus in

this paper will be cases where we investigate the entanglement between two such qubits induced by their interaction with a cavity mode. Another way to restrict excitons to discrete energy levels in 2D is to trap them in harmonic potentials. One way to do this is through pinning the 2D material with a thin needle [16], or to apply a potential difference between two layers of the material [17]. These methods to achieve discrete energy levels for excitons can be applied to various 2D materials, including a class of monolayers of direct band-gap materials, namely, Transition Metal Dichalogenides (TMDCs) [18, 19].

Another important property of graphene is the chirality of its two independent valleys. This leads to the fact that circularly polarized light is absorbed in different valleys, depending on the sign of the circular polarization. In addition, a consequence of the chirality of the valleys is that the pseudomagnetic field arising during deformation has opposite directions in different valleys. As a result of this, the appearance of a pseudomagnetic field during deformation does not contradict the absence of violation of invariance with respect to time reversal in the system in the absence of a real magnetic field.

When graphene is pumped by plane-polarized photons, the absorption of photons occurs in both valleys, accompanied by the appearance of electrons and holes in them. As a result of Coulomb attraction, these electrons and holes form excitons. Moreover, electrons can bind both with holes from their own valley (intravalley excitons) and with holes from another valley (intervalley excitons).

Since the pseudomagnetic field acts in the same way on an electron and a hole, and the pseudomagnetic fields in different valleys have the opposite direction (opposite sign), the spectrum of intervalley pseudomagnetoexcitons, as can be easily shown, turns out to be discrete, in contrast to magnetoexcitons in real magnetic fields. Therefore, intervalley excitons can be used as quantum elements for quantum technologies. A pair of intervalley excitons can be located either in the same pair of graphene valleys, or in different pairs of valleys, and the electrons in each pair of valleys have two choices for holes. Therefore, there are four states for intervalley excitons, which have the same energies and other properties due to the symmetry between the valleys. Thus, intervalley excitons are actually ququarts, which can also be used as intermediate elements in quantum technologies [20]. Note that the properties of the considered ququarts can be controlled using an external real magnetic field.that removes degeneracy and splits levels. This can be used in quantum technologies.

The discrete states for electrons in strained graphene have been studied recently. The zero-temperature semimetal-superconductor (Kekule insulator) transition in graphene and for surface states of topological insulators was analyzed theoretically in Ref. [21]. An experimental study of electron states and the resulting electronic transport properties of uniaxially strained graphene has been reported in Ref. [22]. The theoretical study of electronic edge states in time-periodically driven strained armchair terminated graphene nanoribbons, performed by considering a short-pulse spatial-periodic strain field, has been presented in Ref. [23]. A consistent experimental observation of valley polarization and inversion in strained graphene via pseudo-Landau levels, splitting of real Landau levels, and valley splitting of confined states using scanning tunneling spectroscopy [24]. While in the research mentioned above, the discrete level spectrum for electrons in strained graphene which was analyzed, in this paper we apply the approach, implying the discrete level spectrum for excitons in strained graphene [15], to study the quantum entanglement between two and three excitons treated as two-level systems (qubits). The discrete states for electrons in strained graphene have been studied recently. The zero-temperature semimetal-superconductor (Kekule insulator) transition in graphene and for surface states of topological insulators was analyzed theoretically in Ref. [21]. An experimental study of electron states and the resulting electronic transport properties of uniaxially strained graphene has been reported in Ref. [22]. The theoretical study of electronic edge states in time-periodically driven strained armchair terminated graphene nanoribbons, performed by considering a short-pulse spatial-periodic strain field, has been presented in Ref. [23]. A consistent experimental observation of valley polarization and inversion in strained graphene via pseudo-Landau levels, splitting of real Landau levels, and valley splitting of confined states using scanning tunneling spectroscopy [24]. While in the research mentioned above, the discrete level spectrum for electrons in strained graphene which was analyzed, in this paper we apply the approach, implying the discrete level spectrum for excitons in strained graphene [15], to study the quantum entanglement between two and three excitons treated as two-level systems (qubits).

Quantum entanglement is a degree of bonding which quantum subsystems might have that has no classical counterpart. Since it cannot be created locally (by acting on a single subsystem), but it can be transferred from one subsystem to another, it is usually treated as an important resource in quantum information and quantum computation [25], and, like any useful resource, quantifying it has become an important challenge. Many different ways of measuring the entanglement of a quantum system have been suggested [26–29]. One of those is Concurrence [29], a measure of entanglement between a pair of two-leveled quantum systems, or simply, two qubits.

Recently, the conditional concurrence created by the dynamical Lamb effect of two qubits within a microcavity which changes its frequency suddenly was calculated [30]. In this paper, we find the concurrence created by two

pseudomagnetic excitons on a graphene sheet under strain embedded in a microcavity interacting with one of its modes in the rotating wave approximation (RWA). After that, motivated by the well known work of Greenberger, Horne and Zeilinger [31], where it was shown that the study of the dynamics of quantum systems of more than two elements is enough to prove the validity of quantum mechanics, we do a brief study of the dynamics of the entanglement between three qubits.

The rest of our paper is organized as follows: In Sec. II, we define the system under investigation, which consists of a pair of excitons on a graphene sheet under strain inside an optical microcavity. In Sec. III, we present and solve a model Hamiltonian for the system. Sec. IV is devoted to a study of the entanglement created by the dynamics through calculating the concurrence between the excitons. We study in Sec. V what happens when the system is subject to dissipation. In Sec. VI, we investigate the time evolution of the entanglement between those two excitons. This is accomplished by calculating the time evolution of the concurrence. In Sec VIII, we generalize the model for more than two qubits. In Sec. VII, we apply our model to the case of excitons on a graphene sheet under strain and explain how to generalize the result to other 2D materials. The possible physical realizations for the system under consideration are analyzed in Sec. IX. In Sec. X, we compare our results with those of some recent papers. In Sec. XI, we present a summary of this work.

II. EXCITONS ON A GRAPHENE SHEET UNDER STRAIN

It has been shown that particles on a graphene sheet that is subjected to strain obey a Hamiltonian which is equivalent to one describing the effects of magnetic field [14]. The effect of these so-called pseudomagnetic fields differs from real magnetic fields by the fact that they are charge-independent, affecting positively and negatively charged particles the same way. Strain-induced pseudomagnetic fields in graphene, like external magnetic fields, provide a favorable environment for the formation of excitons, the quasiparticles formed by the bound state of electrons and holes. Within this environment, the resulting excitons, formed by an electron and a hole in different valleys, have a non-dispersive discrete energy spectrum [15]. In contrast, excitons in an applied magnetic field have discrete energy levels each of which is dispersive [3]. The energy eigenvalues for the pseudomagnetoexcitons (PMEs) have been calculated [15] and are given by

$$E_{n,\tilde{n},\tilde{m}} = \varepsilon_{0n,\tilde{n}} + E'_{\tilde{n},\tilde{m}} \ , \tag{1}$$

where, for the simplest case in which the electron and hole masses are the same,

$$\varepsilon_{0n,\tilde{n}} = \hbar\omega_c(n + \tilde{n} + 1). \tag{2}$$

The quantum numbers n and $\tilde{n}$ quantify the cyclotron motion of the center of mass and relative motion, respectively. The term $E'_{\tilde{n},\tilde{m}}$ represents the excitonic binding energy which depends on a new quantum number $\tilde{m}$. Calculated values for the excitonic binding energies $E'_{\tilde{n},\tilde{m}}$ are presented in Ref. [15]. In Eq. (2), the cyclotron frequency ω_c is given by $\omega_c = \dfrac{B}{m}$, where B is the intensity of the pseudomagnetic field ($\frac{B}{e}$ has units of Teslas) and m is the electronic mass.

Since they present a discrete set of energy eigenstates, under suitable conditions, PMEs can be treated as qubits. Here, we consider a system consisting of two such qubits that are coupled to a single cavity mode and study the quantum entanglement between them.

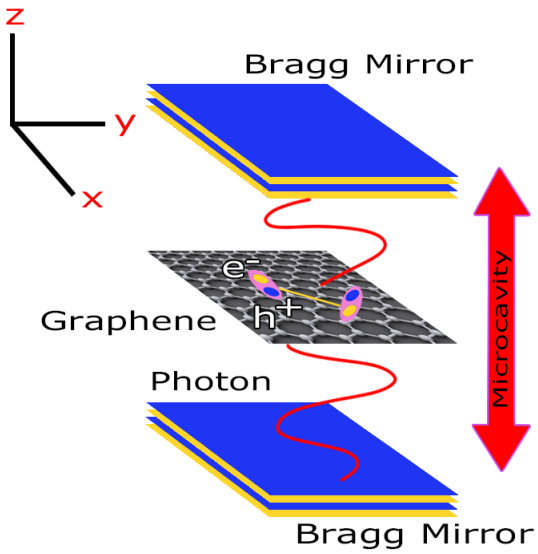

Figure 1: System studied throughout the paper, consisting of 2 excitons on a strained sheet of graphene interacting with a single mode inside an optical microcavity.

From this point forward, we consider a system consisting of two such PMEs, on a strained graphene sheet inside an optical microcavity (Fig. 1). We consider the exciton-exciton interaction to be negligible and the excitons do not interact directly with one another, but both are in contact with the same cavity mode and are allowed to become entangled by such.

III. A JC-LIKE MODEL FOR TWO QUBITS IN A MICROCAVITY

Qubits form the basics for quantum computing, and quantum entanglement is the key resource present in quantum computing that makes it such a powerful tool. Under the right circumstances, we can consider excitons on a graphene sheet under strain to be qubits. Under these conditions, we applied a Jaynes-Cummings-like model to study the quantum entanglement created between two qubits that are coupled to a single cavity mode.

Let us consider a system consisting of two qubits interacting with a cavity mode with Hamiltonian

$$\hat{H} = \hat{H}_0 + \hat{V'}_{RWA} \tag{3}$$

with the unperturbed Hamiltonian $\hat{H}_0$ given by

$$\hat{H}_0 = \hbar \left(\sum_{j=1}^{2} \omega_0 \left| e_j \right\rangle \left\langle e_j \right| + \omega_k \hat{a}^\dagger \hat{a} \right) , \tag{4}$$

where, in this notation, $|e_j\rangle$ is the excited state of qubit j, $\hbar\omega_0$ is the energy gap of the qubits, ω_k is the mode frequency and $\hat{a}^\dagger$ and $\hat{a}$ are the creation and annihilation operators for photons in the cavity. Here, we consider the excited state for the qubit, $|e\rangle$, to consist of an exciton in its first excited state, and $|g\rangle$ to consist of that same exciton in the ground state. Also, for simplicity, in Eq. (4), we relabel the excitonic energies so that the energy of an exciton in the ground state is set equal to 0. The energy gap $\hbar\omega_0$ comes directly from Eq. (1) and is equal to $\hbar\omega_0 = E'_{0,1} - E'_{0,0}$. Therefore, the eigenstates of $\hat{H}_0$ are $|n; ij\rangle$, having energy E_{nij} given by

$$E_{nij} = \hbar[\omega_0(i+j) + n\omega_k] \tag{5}$$

where $i = 1$ ($j = 1$) if the first (second) qubit is in the excited state $|e\rangle$ and $i = 0$ ($j = 0$) if the first (second) qubit is in the ground state $|g\rangle$.

The interaction Hamiltonian on the rotating wave approximation (RWA), $\hat{V'}_{RWA}$ is given by [32]

$$\hat{V'}_{RWA} = \hbar\lambda \sum_{j=1}^{2} \left(\hat{\sigma}_j^+ \hat{a} + \hat{\sigma}_j^- \hat{a}^\dagger\right) \tag{6}$$

where $\hat{\sigma}_j^\pm$ are the creation (+) and annihilation (-) operators for the qubit j and λ is the exciton-photon coupling constant.

This Hamiltonian is similar to that for the Jaynes-Cummings model [33, 34], except that it is for two qubits in one cavity mode. Since the qubits interact with the mode according to the RWA, the destruction (creation) of photons is determined by the creation (annihilation) of qubit excitations. Therefore, as for the Jaynes-Cummings model, we can treat each manifold with fixed number of excitations, meaning the sum of the number of photons and the number of qubit excitations, individually. The n-th manifold is composed of the states with n total excitations, namely $|n; 00\rangle \equiv |0_n\rangle$, which is the state with n cavity photons and no qubit excitations; $|n-1; 01\rangle \equiv |1_n\rangle$, the state with $n-1$ cavity photons and with qubit "1" in the excited state $|e\rangle$; $|n-1; 10\rangle \equiv |2_n\rangle$, the state with $n-1$ cavity photons and with the qubit "2" in the excited state $|e\rangle$ and $|n-2; 11\rangle \equiv |3_n\rangle$, the state with $n-2$ total excitations and both qubits in the excited state. It is important to note that each manifold is 4-dimensional with exception to the $n = 1$, which is 3-dimensional and to the $n = 0$ which is composed only with the ground state, $|0; 00\rangle$. The effective Hamiltonian, $\hat{H}_n$, on the n-th manifold appears directly from Eq. (3) and is equal to

$$H_1 = \hbar \begin{pmatrix} \omega_k & \lambda & \lambda \\ \lambda & \omega_0 & 0 \\ \lambda & 0 & \omega_0 \end{pmatrix}, \tag{7}$$

for $n = 1$ and

$$H_n = \hbar \begin{pmatrix} n\omega_k & \lambda\sqrt{n} & \lambda\sqrt{n} & 0 \\ \lambda\sqrt{n} & (n-1)\omega_k + \omega_0 & 0 & \lambda\sqrt{n-1} \\ \lambda\sqrt{n} & 0 & (n-1)\omega_k + \omega_0 & \lambda\sqrt{n-1} \\ 0 & \lambda\sqrt{n-1} & \lambda\sqrt{n-1} & (n-2)\omega_k + 2\omega_0 \end{pmatrix}, \tag{8}$$

when $n = 2, 3, \cdots$. For the ground state, $H\,|0; 00\rangle = 0$. One can find in a straightforward way the energy eigenstates for the Hamiltonian in (7). The eigenvalues of (7) are

$$\begin{aligned} \epsilon_0 &= \omega_0 \\ \epsilon_\pm &= \frac{1}{2}\left((\omega_0 + \omega_k) \pm \sqrt{(\omega_0 - \omega_k)^2 + 8\lambda^2}\right), \end{aligned} \tag{9}$$

with eigenvectors

$$\begin{aligned} |\psi_0\rangle &= \frac{1}{\sqrt{2}}\left(|0; 01\rangle - |0; 10\rangle\right) \\ |\psi_\pm\rangle &= \frac{1}{\sqrt{2 + a_\pm^2}}\left(a_\pm\,|1; 00\rangle - |0; 01\rangle - |0; 10\rangle\right), \end{aligned} \tag{10}$$

where $a_\pm$ is given by

$$a_\pm = \frac{1}{2\lambda}\left[(\omega_0 - \omega_k) \pm \sqrt{(\omega_0 - \omega_k)^2 + 8\lambda^2}\right]. \tag{11}$$

The eigenvalues and eigenvectors of (8), however, are much more difficult to obtain. However, this problem is solved when we consider the resonance case where the cavity frequency is the same as the qubit transition frequency, $\omega_0 = \omega_k \equiv \omega$. In this case, Eqs. (7) and (8) become

$$H_1 = \hbar \begin{pmatrix} \omega & \lambda & \lambda \\ \lambda & \omega & 0 \\ \lambda & 0 & \omega \end{pmatrix} \tag{12}$$

$$H_n = \hbar \begin{pmatrix} n\omega & \lambda\sqrt{n} & \lambda\sqrt{n} & 0 \\ \lambda\sqrt{n} & n\omega & 0 & \lambda\sqrt{n-1} \\ \lambda\sqrt{n} & 0 & n\omega & \lambda\sqrt{n-1} \\ 0 & \lambda\sqrt{n-1} & \lambda\sqrt{n-1} & n\omega \end{pmatrix} . . \tag{13}$$

The eigenvalues of (12) are

$$\begin{aligned} \epsilon_0 &= \omega \\ \epsilon_\pm &= \omega \pm \sqrt{2}\lambda, \end{aligned} \tag{14}$$

with eigenvectors

$$|\psi_0\rangle = \frac{1}{\sqrt{2}} \left(|0;01\rangle - |0;10\rangle \right) \tag{15}$$

$$|\psi_\pm\rangle = \frac{1}{2} \left(\pm\sqrt{2}\,|1;00\rangle - |0;01\rangle - |0;10\rangle \right), \tag{16}$$

which are simply Eqs. (9-10) at resonance.

The eigenvalues of Eq. (13) are given by

$$\epsilon_{n0} = n\omega \tag{17}$$

$$\epsilon_{n\pm} = n\omega \pm \sqrt{2(2n-1)}\lambda \ , \tag{18}$$

where the first eigenvalue is doubly degenerate. The corresponding eigenvectors are as follows

$$|\psi_{n0,1}\rangle = \frac{1}{\sqrt{2}}(|n-1;01\rangle - |n-1;10\rangle) \tag{19}$$

$$|\psi_{n0,2}\rangle = \frac{1}{\sqrt{2n-1}} \left(\sqrt{n-1}\,|n;00\rangle - \sqrt{n}\,|n-2;11\rangle \right) \tag{20}$$

$$|\psi_{n\pm}\rangle = \frac{1}{\sqrt{8n-4}} \left[\sqrt{2n}\,|n;00\rangle + \sqrt{2(n-1)}\,|n-2;11\rangle \pm \sqrt{2n-1}\,(|n-1;01\rangle + |n-1;10\rangle) \right] \ . \tag{21}$$

Here, $|\Psi_{n0,1}\rangle$ and $|\Psi_{n0,2}\rangle$ are the two degenerate eigenstates with eigenvalue ϵ_{n0} and $|\psi_{n\pm}\rangle$ are the eigenstates corresponding to the eigenvalue $\epsilon\pm$. It is interesting to note that the eigenvalues and eigenvectors of Eqs. (12) and (13) do agree with each other for the case $n = 1$, with the exception of the eigenvector $|\psi_{n0,2}\rangle$, which, for $n = 1$, contains a vector that does not exist in reality, corresponding to a state with 1 photon, as can be readily seen from Eq. (20).

IV. CONCURRENCE FOR ENERGY EIGENSTATES

Now that we have the energy eigenstates for the Hamiltonian, we can determine the quantum entanglement for each of them. The most used measure for quantum entanglement between two qubits is the concurrence [25] which is what we employ here. We can use Eq. (19-21) to determine the concurrence between a pair of qubits in energy eigenstates for all $n > 1$ and Eqs. (15) and (16) to calculate the concurrence for all energy eigenstates corresponding to $n = 1$. The concurrence for a pair of qubits in state $|\psi\rangle = a\,|00\rangle + b\,|11\rangle + c\,|10\rangle + d\,|01\rangle$, where $\langle\psi|\psi\rangle = 1$ is given by [25]

$$C(\psi) = 2|ab - cd| \ . \tag{22}$$

For a mixed state with density matrix ρ, the concurrence of the system is defined by [29]

$$C = \max\{0, \lambda_1 - \lambda_2 - \lambda_3 - \lambda_4\} \ , \tag{23}$$

where λ_i are the eigenvalues in descending order of $\tilde{\rho}\rho$. The matrix $\tilde{\rho}$ is the result of applying the spin-flip operator to ρ so that

$$\tilde{\rho} = (\sigma_y \otimes \sigma_y)\rho^*(\sigma_y \otimes \sigma_y) \ . \tag{24}$$

By substituting Eq. (19-21) in Eq. (22), we obtain the concurrence for the $n > 1$ energy eigenstates to be

$$\begin{aligned} C(\psi_{n0,1}) &= 1 && n \geq 1 \\ C(\psi_{n0,2}) &= \frac{2n\sqrt{1-\frac{1}{n^2}}}{2n-1} && ; n \geq 2 \\ C(\psi_{n\pm}) &= \frac{\left|1 - 2n\left(1 - \sqrt{1-\frac{1}{n^2}}\right)\right|}{4n-2} && ; n \geq 1 \ . \end{aligned} \tag{25}$$

Also, for $n = 1$, we substitute Eqs. (15) and (16) into Eq. (22) to find

$$\begin{aligned} C(\psi_0) &= 1 \\ C(\psi_\pm) &= \frac{1}{2} \ . \end{aligned} \tag{26}$$

It is interesting to note that, in the case when there is resonance, the concurrence does not depend on any of the system parameters (i.e., the energy gap ω and the coupling strength λ). The concurrence of an eigenstate of the Hamiltonian which is in a superposition of $|\psi_{n0,1}\rangle$ and $|\psi_{n0,2}\rangle$ such as $|\Psi\rangle = \frac{1}{\sqrt{|a|^2+|b|^2}}\left(a\,|\psi_{n0,1}\rangle + b\,|\psi_{n0,2}\rangle\right)$ is given by

$$C(\Psi) = \frac{1}{|a|^2+|b|^2}\left|a^2 - b^2\frac{2n\sqrt{1-\frac{1}{n^2}}}{2n-1}\right| \tag{27}$$

which can vary continuously between 0 and 1.

If the system is off resonance for the states represented by Eq. (10) or (11), the concurrence will be equal to

$$\begin{aligned} C(\psi_0) &= 1 \\ C(\psi_\pm) &= \frac{2}{2+a_\pm^2}, \end{aligned} \tag{28}$$

where $a_\pm$ is given by Eq. (11). We see that in this case the concurrence depends only on the dephasing $(\omega_0 - \omega_k)$ and on the coupling strength between the qubits and a cavity mode photon, λ, but not on the individual frequencies ω_0 and ω_k. It is reasonable to expect that the same will be true for $n > 1$.

V. DISSIPATIVE SYSTEM

So far, we have considered ideal systems that do not interact with the environment. For those systems, the quantum entanglement is preserved, not decaying with time. However, real systems experience various forms of dissipation that end up destroying the entanglement between the qubits. In this section, we study the dynamics of the same system as described above , but now in the presence of dissipation, in order to see how the concurrence (and, with it, the quantum entanglement) evolves in time.

From this point onward, we assume that this system is not isolated and, therefore, it suffers dissipation. When a system experiences any form of dissipation, its time evolution ceases to obey Schrödinger's equation. The most common forms of dissipation force the system to evolve under a master equation such as [35]

$$\dot{\rho} = -i[\hat{H}, \rho] + \kappa\mathcal{L}(\hat{a})\rho + \sum_{j=1}^{2}\left(\gamma\mathcal{L}(\hat{\sigma}_j^-)\rho + \gamma_\phi\mathcal{L}\left(\hat{\sigma}_j^{(3)}\right)\rho\right), \tag{29}$$

where ρ is the system's density matrix, the Lindblad operators $\mathcal{L}$ are defined as [35]

$$\mathcal{L}(\hat{A})\rho = \hat{A}\rho\hat{A}^\dagger - \frac{1}{2}\left(\hat{A}^\dagger\hat{A}\rho + \rho\hat{A}^\dagger\hat{A}\right) \ , \tag{30}$$

and κ, γ and γ_ϕ represent possible channels of dissipation representing, respectively, the cavity relaxation, qubit relaxation and qubit dephasing.

First, let us consider the effect due to each term of Eq. (29). The Schrödinger term ($i[H, \rho]$) neither creates nor destroys excitations, it can only transform a photon on an excitation on either qubit or transform an excitation on either qubit into a photon, the Lindblad terms can only destroy excitations or simply dephase the system. This means that, if we start with a system with a maximum value for n total excitations, we need only to concern ourselves with matrix elements between states with n or less total excitations, because neither term in the master equation is able to create excitations, only interchange them or destroy them. In particular, if we are interested in systems with one excitation, we need only treat matrix elements between the states $|0;00\rangle \equiv |0\rangle$, $|0;10\rangle \equiv |1\rangle$, $|0;01\rangle \equiv |2\rangle$ and $|1;00\rangle \equiv |3\rangle$, where this relabeling was made for a cleaner notation. In this case, we can write the density matrix $\rho(t)$ as [32]

$$\rho(t) = \sum_{i,j=0}^{3}\rho_{ij}(t)\,|i\rangle\langle j| \ , \tag{31}$$

where the matrix elements obey the usual conditions, i.e., $\rho_{ij} = \rho_{ji}^*$, $0 \leq \rho_{ii} \leq 1$ and $\sum_i \rho_{ii} = 1$. Substituting (31) into (42), we find

$$\begin{aligned}\dot{\rho}_{ij} &= -i\langle i|\left[\hat{H}, \rho\right]|j\rangle + \langle i|\left[\kappa\mathcal{L}(\hat{a})\rho + \sum_{j=1}^{2}\left(\gamma\mathcal{L}(\sigma_j^-)\rho + \gamma_\phi\mathcal{L}\left(\sigma_j^{(3)}\right)\right)\right]\rho\,|j\rangle \\ &= \dot{\rho}_{Sij} + \dot{\rho}_{\mathcal{L}_{ij}} \ ,\end{aligned} \tag{32}$$

where

$$\begin{aligned}\dot{\rho}_{Sij} &= -i\langle i|\left[\hat{H}, \rho\right]|j\rangle \\ \dot{\rho}_{\mathcal{L}_{ij}} &= \langle i|\left[\kappa\mathcal{L}(\hat{a})\rho + \sum_{j=1}^{2}\left(\gamma\mathcal{L}(\sigma_j^-)\rho + \gamma_\phi\mathcal{L}\left(\sigma_j^{(3)}\right)\right)\right]\rho\,|j\rangle\,.\end{aligned} \tag{33}$$

In the low-temperature regime, we neglect the effect due to phonons on the properties of the graphene sheet and the decay of the system is governed by the cavity decay. In this regime, we have $\gamma = \gamma_\phi = 0$. Equation (32) gives rise to a set of ten independent, linear differential equations that are dealt with in Appendix for the case where the main

form of dissipation is through cavity decay. In the Appendix, we focus our attention on the steady states, which are preserved by the dynamics and on finding the differential equations that govern the dynamics for each element of the density matrix. The non-trivial steady state is found in equations (A19) and (A20). The differential equation system (A14) was then used to create a program that simulates the dynamics.

There are mainly two important results taken from the solution in Eq. (32). The first one is that when dissipation comes mainly from cavity decay, meaning that at low temperature T, the maximum entangled Bell state $|0;\Psi_-\rangle$,

$$|0;\Psi_-\rangle = \frac{1}{\sqrt{2}}\left(|0;10\rangle - |0;01\rangle\right) \tag{34}$$

is a steady state and does not decay into the ground state. Another is that the characteristic decay time for all other states is of the order of $\tau = 1/\kappa$, as it should be expected.

VI. CONCURRENCE AS A FUNCTION OF TIME

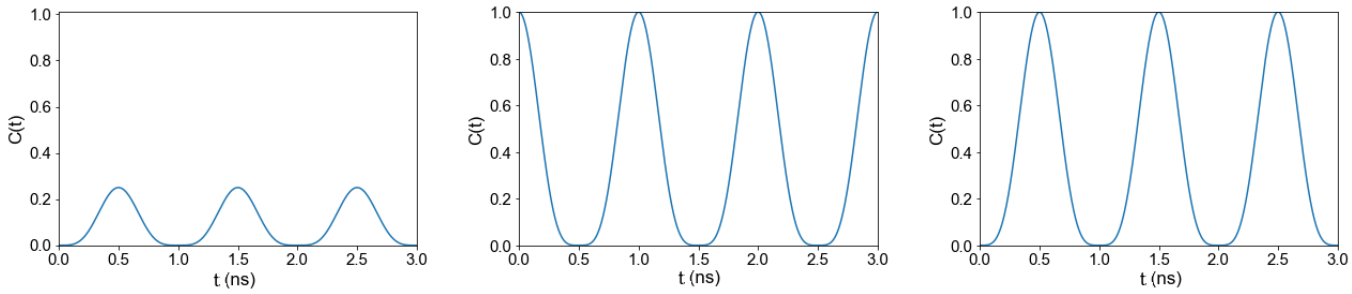

(a) (b) (c)

Figure 2: Concurrence between two qubits as a function of time for a system with no dissipation for four different initial states (a) $\rho_0 = |0;10\rangle\langle 0;10|$, meaning the first qubit starts in the excited state and the second in the ground state; (b) $|0;\Psi_+\rangle\langle 0;\Psi_+|$, the maximally entangled state that is not an eigenstate of Eq. (3); and (c) $|1;00\rangle\langle 1;00|$, both qubits originally from the ground state and the cavity with a single photon.

As it was shown, the dynamics of a system that evolves under a master equation such as Eq. (32) intertwines the states of both qubits. This means that one should expect the concurrence between those qubits to be a function of time. At low temperature, the system can only decay through the loss of cavity photons. In this case, the only two steady states are the ground state, $|g\rangle = |0;00\rangle$, which has no concurrence ($C = 0$) and the state $|0;\Psi_-\rangle$, given by Eq. (34).

A computer program that simulates the time evolution of a system governed by equation (A14) was written and both the concurrence and probability for the system to decay to the ground state were calculated as a function of time. For all the simulations shown in this session, we chose the Rabi frequency to be $\frac{2\pi}{2\sqrt{2}}\text{ns}^{-1}$.

We start with Fig. 2 which presents the evolution of the concurrence as a function of time for a system with no dissipation ($\kappa = 0$). The effect of the dynamics is such that it creates oscillations between states $|0;\Psi_+\rangle$ and $|1;00\rangle$ with frequency $\omega = 2\sqrt{2}\lambda$. The maximally entangled state $|0;\Psi_-\rangle$, which has concurrence $C = 1$, is a steady state that has been omitted from the figure for better visualization of the non-trivial cases. The result is that the concurrence as a function of time presents oscillations between a maximum and minimum value that depends on the initial state. However, the most interesting result appears when we take dissipation into account. Figs. 3 and 4 show what happens with such systems for two different initial states.

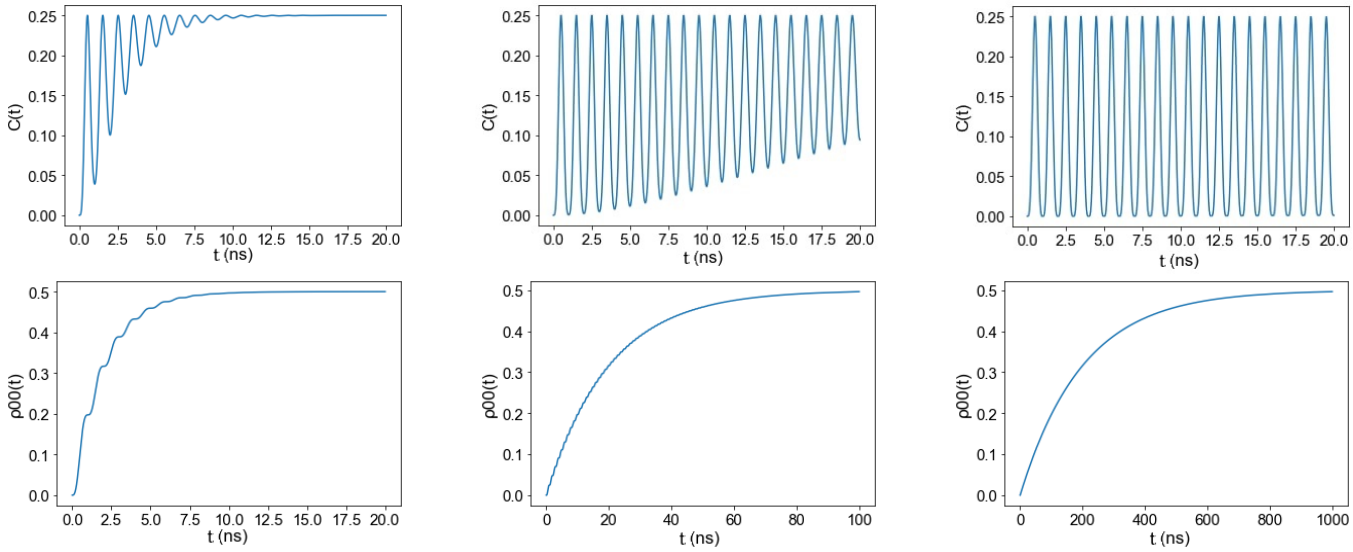

(a) (b) (c)

Figure 3: In the first row, concurrence between two qubits as a function of time for a system with dissipation for three different values of κ: (a) $\kappa = 1\text{ns}^{-1}$; (b) $\kappa = 0.1\text{ns}^{-1}$ and (c) $\kappa = 0.01\text{ns}^{-1}$. In the second row, we have the probability for the system to decay to the ground state as a function of time. In these simulation, the initial state of the system is always state $\rho_0 = |0;10\rangle\langle 0;10|$.

Fig. 3 shows how the concurrence evolves as a function of time for a system originally with one qubit in the excited state and one in the ground state for different cavity decay rates κ, while Fig. 4 shows the same information for a system originally in the maximally entangled Bell state $|0;\Psi_+\rangle$. The interesting thing to note is that although for the one in Fig. 4 the concurrence eventually decay to zero as the system decays to the ground state with probability one, for the initial state represented in Fig. 3, the decaying process actually increases the concurrence as time passes, and the decay probability goes to 0.5.

The expression for $\rho(t_0)$ is given by

$$\rho(t_0) = \rho_0 |\psi_0\rangle\langle\psi_0| + \rho_+ |\psi_+\rangle\langle\psi_+| + \rho_- |\psi_-\rangle\langle\psi_-| + \sum_{i\neq j} \rho_{ij} |\psi_i\rangle\langle\psi_j| + \rho_g |0;00\rangle\langle 0;00| \ , \tag{35}$$

where, as in Eq (10), $|\psi_0\rangle = |0;\Psi_-\rangle$ and the sum is taken over $i, j = +, -$ and 0. The effect of the master equation on this basis is to keep ρ_0 constant while slowly of all other terms on the first manifold (all ρ_{ij}'s along with $\rho_\pm$) and increasing the probability for the system to be found on the ground state, ρ_g. The system will asymptotically decay to the final state

$$\rho(t\to\infty) = \rho_0 |\psi_0\rangle\langle\psi_0| + (1-\rho_0) |0;00\rangle\langle 0;00| \ . \tag{36}$$

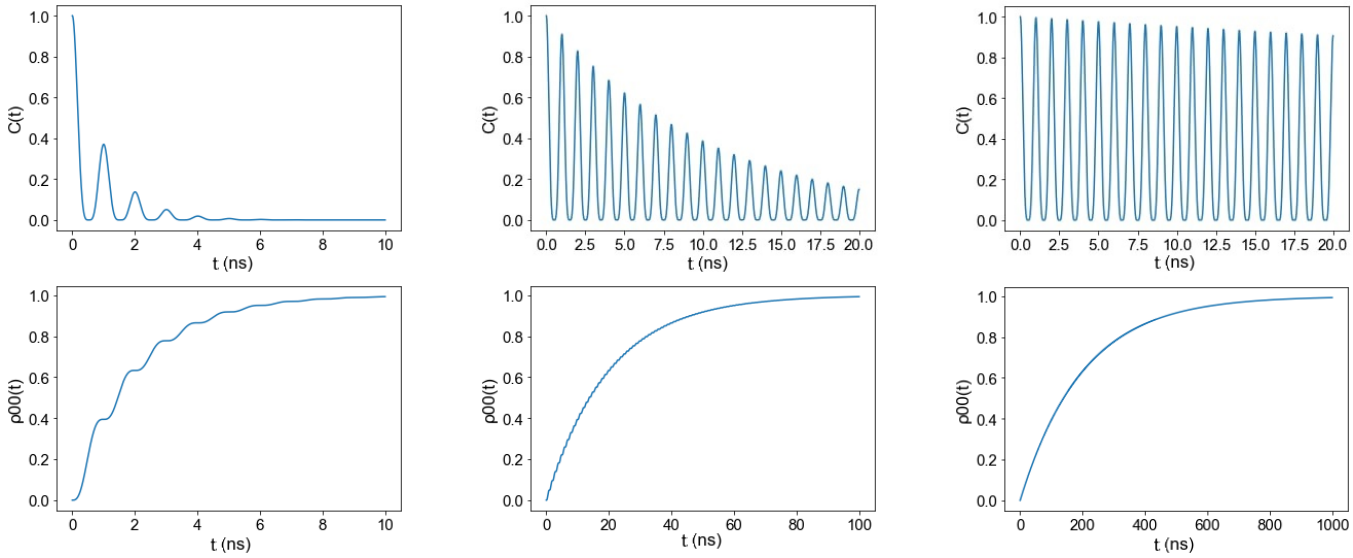

Figure 4: The first row displays the concurrence between two qubits as a function of time for a system with dissipation for three different values of κ: (a) $\kappa = 1\text{ns}^{-1}$; (b) $\kappa = 0.1\text{ns}^{-1}$ and (c) $\kappa = 0.01\text{ns}^{-1}$. In the second row, we have the probability for the system to decay to the ground state as a function of time. In these simulations, the initial state of the system is always state $\rho_0 = |0;\Psi_+\rangle\langle 0;\Psi_+|$.

When the system reaches the state represented in Eq. (36), the concurrence can be calculated in a straightforward way by Eq. (23) and found to be

$$C(t \to \infty) = \rho_0^2, \tag{37}$$

which is nothing more than the square of the probability for the system to be found in the maximally entangled Bell state $|0;\Psi_-\rangle$, defined in Eq. (34). The time which the system takes to decay to such a state is clearly dependent on the decay rate κ of the cavity, but the final state only depends on the initial state. This means that, in some cases, concurrence can be protected from, *and even created by*, dissipation in the system. This protection from decay comes from the fact that we are considering that the system can only decay through the emission of cavity photons and there exists an eigenstate of the Hamiltonian in which there are no cavity photons.

VII. CONCURRENCE BETWEEN EXCITONS ON A GRAPHENE SHEET UNDER STRAIN

We can now combine the results obtained in the previous sections to properly calculate the entanglement for our system of interest. In order to do so, we consider the same system as that in Ref. [15], which is that for a graphene sheet under a strain-induced magnetic field of magnitude $\frac{B_z}{e} = 50\ T$, embedded in a GaAs microcavity with dielectric constant $\varepsilon = 13$. Assuming that the system is in resonance with the cavity, we need only to find the value of the Rabi splitting in order to calculate the time evolution of the concurrence between the excitons.

The Rabi splitting for excitons in graphene under a high magnetic field inside an optical microcavity has been calculated and found to be [36]

$$\hbar\lambda = e\left(\frac{\hbar\pi v_F r_B}{\sqrt{2}\epsilon W}\right)^{\frac{1}{2}}, \tag{38}$$

where e is the electronic charge, $r_B = \sqrt{\hbar/B_z}$ is the magnetic length for chosen magnetic field B_z, ϵ is the dielectric constant of the cavity, v_F is the Fermi velocity for electrons in graphene and W is the cavity's volume. The calculations in Ref. [36] that led to Eq. (38) depended only on a single electron wave function and on the fact that the

excitonic binding energy was much smaller than the band gap. The single electron wave function for an electron in a pseudomagnetic field is completely isomorphic to that of an electron in an external magnetic field and the excitonic binding energy is also much smaller than the gap. This means that the Rabi splitting for excitons on a graphene sheet under strain is the same as the one for excitons on a graphene sheet in high magnetic field and is also given by Eq. (38). Choosing the intensity of the strain-induced pseudomagnetic field as $\frac{B_z}{e} = 50\ T$, a number that has been achieved experimentally for carbon nanotubes [14], the Fermi velocity for electrons in graphene to be $v_F = 10^6 m/s$ and a GaAs microcavity ($\varepsilon = 13$) of volume $W = 1.69 \times 10^3 \mu m^3$ [37], the Rabbi splitting becomes $\hbar\lambda = 0.027$ meV. The time evolution of the mean value of the concurrence was calculated for such a system that is inside a medium quality cavity, where photons have a medium lifetime of 1 μs ($\kappa = 10^{-3} ns^{-1}$). Those results are shown in Fig. 5 for many different initial states. The initial states $|\Psi_0\rangle$ considered in Fig. 5 for $t = 0$ could be prepared, for example, by creating the excitons by irradiating a precise femtosecond laser pump on the graphene sheet.

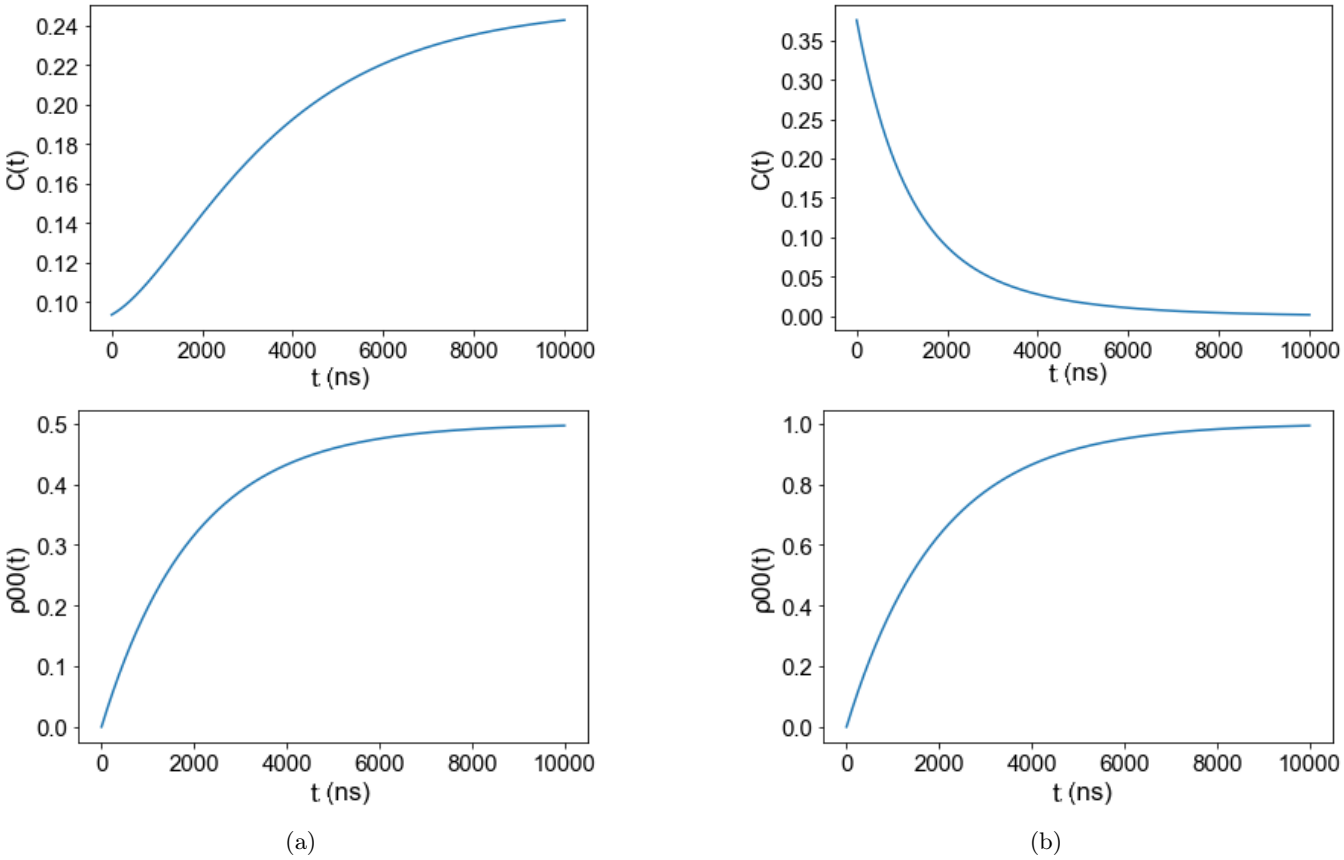

(a) (b)

Figure 5: In the first row, the concurrence between a pair of qubits averaged in a single Rabi cycle as a function of time for a system with dissipation for three chosen initial states $|\Psi_0\rangle$: (a) $|\Psi_0\rangle = |0; 10\rangle$; and (b) $|\Psi_0\rangle = |0; \Psi_+\rangle$. The second row shows the probability for the system decaying to the ground state as a function of time.

Figure 5 shows that the effect due to cavity decay is not always the one which might seem intuitive, i.e., destroying the concurrence between excitons. This may be true if the system starts with no component in the Bell state $|0; \Psi_-\rangle$, when written in Bell's basis. However, if there are components on this basis vector, the final concurrence will not be zero and can occasionally even increase with time due solely to the fact that the cavity decays. The maximally entangled steady state $|0; \Psi_-\rangle$, that has concurrence $C = 1$ and has zero probability to decay to the ground state has been omitted from the figure for better visualization. For such systems, the concurrence between two PMEs can be preserved throughout the entire lifetime of the excitons on graphene which, at low temperatures, can be a very long time since in this regime, excitons can only decay by photon emission and the $|0; \Psi_-\rangle$ state is protected from such decay. Even though we considered excitons on a graphene sheet under strain throughout this paper, the same results apply to any excitonic system in which excitons have a set of discrete energy levels. One such example is for trapped excitons on a TMDC monolayer or bilayer. One can make such a trap by, for example, pinning the TMDC with a thin needle [16] or by applying a potential difference between two layers at a given point [17].

VIII. THE 3-QUBITS CASE

In order to check whether a system with more than two qubits embedded in a single cavity mode would yield similar results, we now carry out a brief study of the three-qubit system. A system of three qubits in resonance with a single cavity mode will obey a Hamiltonian

$$\hat{H} = \hat{H}_0 + \hat{V}'_{RWA} \tag{39}$$

with the unperturbed Hamiltonian $\hat{H}_0$ given by

$$\hat{H}_0 = \hbar\omega_0 \left(\sum_{j=1}^{3} |e_j\rangle \langle e_j| + \hat{a}^\dagger \hat{a} \right) , \tag{40}$$

and the interaction in the RWA $\hat{V}'_{RWA}$

$$\hat{V}'_{RWA} = \hbar\lambda \sum_{j=1}^{3} \left(\hat{\sigma}_j^+ \hat{a} + \hat{\sigma}_j^- \hat{a}^\dagger \right) . \tag{41}$$

As for the one and two-qubit case, this Hamiltonian divides the system's Hilbert space into manifolds with the same total number of excitations. The manifold for $n = 1$ total excitations is composed of the states $|1;000\rangle$, $|0;100\rangle$, $|0;010\rangle$ and $|0;001\rangle$. Similar to the two qubit case, in the presence of dissipation, the system will evolve under a Master equation of the form [35]

$$\dot{\rho} = -i[\hat{H}, \rho] + \kappa \mathcal{L}(\hat{a})\rho \tag{42}$$

with the Lindblad operator $\mathcal{L}(\hat{a})\rho$ defined by Eq. (30). In Fig. 6, we evaluated the probability for such a system to decay to the ground state as a function of time for chosen initial states.

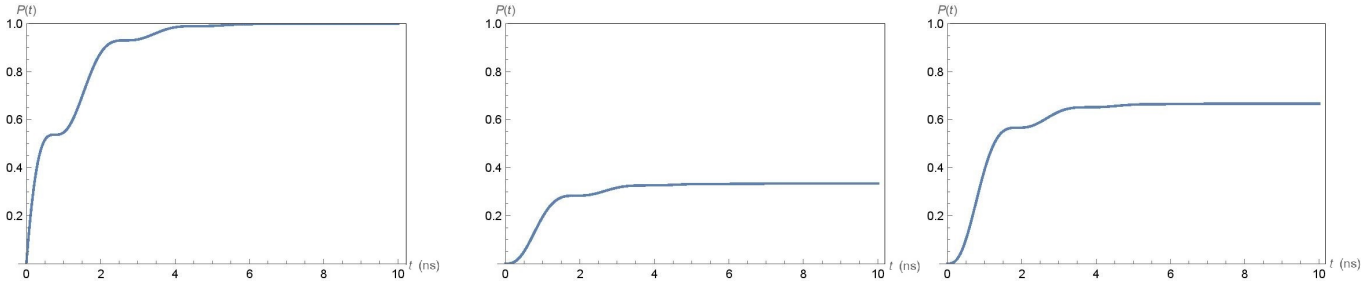

(a) (b) (c)

Figure 6: Probability $P(t)$ for a three qubit system to decay to the ground state $|0;000\rangle$ as a function of time for $\hbar\lambda = \kappa = 1$ ns^{-1} for various initial states. (a) $\rho_0 = |1;000\rangle \langle 1;000|$; (b) $\rho_0 = |0;100\rangle \langle 0;100|$; (c) $\rho_0 = |\Psi_+\rangle \langle \Psi_+|$, where $|\Psi_\pm\rangle = \frac{1}{\sqrt{2}} (|0;100\rangle \pm |0;010\rangle)$.

In Fig. 6, we can see that just as for the two-qubit case, the system does not decay to the ground state with probability one for all initial states. Again, there exists a maximally entangled state $|\Psi_-\rangle = \frac{1}{\sqrt{2}} (|0;100\rangle - |0;010\rangle)$ which has zero probability for it to decay and was omitted from the figure for a clearer presentation. We can assume that, just like for the two qubits case, the fact that the system does not decay with probability one means that some quantum entanglement is preserved. Additionally, by looking at Fig. 6 (b), which starts in an originally pure and un-entangled state, at least for that case, the average amount of quantum entanglement in the system it is enhanced by the possibility for the system to decay.

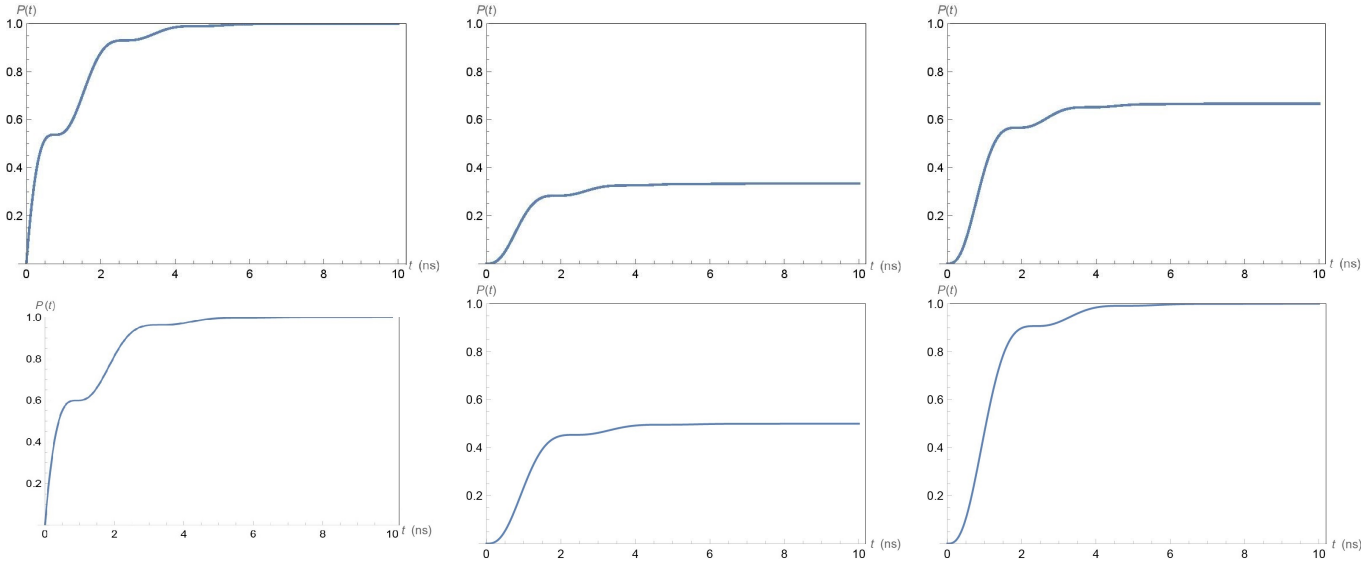

Figure 7: Probability $P(t)$ for a three qubit system (upper row) or a two qubit system (lower row) to decay to the ground state ($|0;000\rangle$ for three qubits, or $|0;00\rangle$ for two) as a function of time for $\hbar\lambda = \kappa = 1$ ns^{-1} for various initial states. (a) The system starts with no qubit excitations and one cavity photon; (b) The system starts with no cavity photons, one qubit in the excited state and all others in the ground state; (c) The system starts with no cavity photons and one pair of qubits in the maximunly entangled Bell state $|\Psi_+\rangle$.

In Fig. 7, we compare our results for the dynamics for two and three qubits, by analyzing the decay probability for equivalent initial states in both cases. As it can be seen from the figures, the time it takes for the system to thermalize is independent of the number of qubits. We can also see that the probability for the three-qubit system to remain in an exited state after thermalization and, therefore, present some degree of entanglement, is always equal or greater than that for the two-qubit system, for equivalent initial states. This probability is equal for the cases in which the system starts either in a state with one photon in the cavity and no excitations of the qubits, or the system starts with two qubits in the maximally entangled Bell state $|\Psi_-\rangle$. For the cases in which the system starts with no cavity photons and a single excited qubit or no cavity photons and a pair of qubits in the maximally entangled Bell state $|\Psi_+\rangle$, the three-qubit system is less likely to decay than the ywo-qubit one. One can understand this fact by noting that for three qubits, there are actually two linearly independent eigenstates of the original Hamiltonian with no cavity photons, namely $|\Psi_{-_{1,2}}\rangle = \frac{1}{\sqrt{2}}(|0;100\rangle - |0;010\rangle)$ and $|\Psi_{-_{1,3}}\rangle = \frac{1}{\sqrt{2}}(|0;100\rangle - |0;001\rangle)$ ($|\Psi_{-_{2,3}}\rangle = \frac{1}{\sqrt{2}}(|0;010\rangle - |0;001\rangle)$ is also an eigenstate, but it is LD of the previous two since it can be written as $|\Psi_{-_{2,3}}\rangle = |\Psi_{-_{1,3}}\rangle - |\Psi_{-_{1,2}}\rangle$). This means that there is an additional stable state that the system can remain in as $t \to \infty$. This is the reason why the probability for the system to remain entangled is greater for the higher qubit count.

IX. POSSIBLE PHYSICAL REALIZATIONS

The following physical realizations are possible for similar qubits based on intervalley excitons: First, for pristine (or gapless) graphene with donor impurities or due to the control electrode, the chemical potential will be in the upper (conductivity) band. Then a magnetic transition is possible between Landau levels in the same conduction band. This transition requires pumping with terahertz photons. As a result of pumping by terahertz photons with linear polarization, intervalley excitons will arise. Secondly, in pristine graphene, pumping by photons in the optical region of the spectrum is necessary, which transfers electrons from the filled Landau level in the valence band to an unfilled Landau level in the conduction band.

Note that the results of this work are valid not only for inter-valley excitons in graphene in a pseudomagnetic field, but also for excitons in other physical systems with a discrete spectrum. For example, one can use excitons in a TMDC material in a 2D trap created by the deformation potential from the tip of a scanning probe microscope.

Another option is a system of Frenkel excitons in 2D organic materials. For efficient control of such qubits and their use in quantum technologies, these systems can be placed in a spatially limited optical cavity with a discrete photon spectrum with resonant frequencies for qubits.

The most important property of qubits used in quantum technologies is quantum entanglement, and no entanglement occurs during adiabatic changes in the system of qubits. For entanglement, a non-adiabatic effect is necessary. With such an effect, interesting phenomena also arise in quantum electrodynamics in a cavity such as the dynamic Lamb effect (see Refs. [30, 38] and references therein). In fact, quantum entanglement should appear immediately upon the above-described appearance of intervalley excitons after pumping with linearly polarized light. Similarly, quantum entanglement of qubits should appear immediately after the pumping of excitons in the trap or pumping of Frenkel excitons. Calculating the properties of such quantum entanglement and its time dependence is the goal of our work. Modern quantum technologies and the prospects for their development are based on the use of quantum two-level systems, i.e., qubits.

Principally new properties of 2D systems arise in pseudomagnetic fields, which arise, in particular, in graphene under strain. This is due to the fact that the effect of pseudomagnetic fields does not depend on the sign of the charge and is the same for electrons and holes.Another important property of graphene is the chirality of only two independent valleys, which leads to the fact that circularly polarized light is absorbed in different valleys of graphene, depending on the sign of circular polarization. Additionally, the consequence of chirality is that the resulting pseudomagnetic field during deformation has a different sign in different valleys. Consequently, the appearance of a pseudomagnetic field due to deformation of graphene does not contradict the absence of violation of invariance with respect to time reversal contrary to the case of graphene in real magnetic field.

If graphene is pumped by plane polarized photons, they are absorbed in both valleys, accompanied by the appearance of electrons and holes in them. As a result of the Coulomb attraction, these electrons and holes form excitons not only in the same valley but also from different valleys. They are more stable due to forbidden luminescence as a consequence of the law of energy and momentum conservation. Consequently, intervalley pseudomagnetoexcitons have discrete spectra and can be used as quantum elements in quantum technologies.

X. DISCUSSION

The model which is studied here bears clear similarities with the well studied double Jaynes-Cummings model, where two entangled qubits are each placed within a well-defined cavity mode. The time evolution for the entanglement for such a system has been thoroughly investigated in the past by other research groups [39–41]. Additionally, it is important to emphasize the key difference between that model and ours. In our model, two qubits that may or may not be initially entangled, are both inserted into a single cavity mode. This system has been briefly described by Casanova *et al.* [42], but, since it was not the main focus of their work, they did not provide details of its dynamics. In the system under consideration in our paper, entanglement can be created or destroyed, depending on the system's original state.

Another important comment is the generality of our model. Here, we applied our results to a system of excitons on a graphene sheet under strain, but, in reality, any physical structure that can be approximated as a two-level system might be used to study the model presented here. This generality might lead to verification of the model in many different physical setups.

XI. CONCLUDING REMARKS

In this paper, we have investigated quantum entanglement between a pair of excitons, formed by an electron and a hole from different valleys in a graphene monolayer under strain within an optical microcavity. We first developed a Jaynes-Cummings like model for two qubits coupled to a single cavity mode which governs the system in the rotating wave approximation (RWA). We then calculated the energy eigenstates of such a model. We measured the degree of entanglement of such states by calculating the concurrence between the two qubits in each of these eigenstates. It was shown that if the system is allowed to decay only through the emission of cavity photons, which is the case at low temperatures, there is a maximally entangled eigenstate which is protected from decay.

We have shown that the existence of such a state leads to the counter-intuitive consequence that, for some initial states of the system, the fact that the cavity is leaky can actually lead to an increase in the average concurrence on

timescales of the average photonic lifetime. After that, by analyzing the three-qubit version of the model, we have not only shown that these results also hold for multi-qubits, but also exhibited evidence that the initial-state-dependent protection for quantum entanglement from decay appears to increase with the number of qubits. Lastly, we used the energy eigenfunctions and eigenvalues for PMEs obtained in Ref. [15] to formally calculate the time evolution of the concurrence between two PMEs in graphene. In addition, we have discussed the applicability of our approach for different 2D materials, such as TMDC monolayers. A worthy next step for this research will be to study in greater depth the three-qubit model. Specifically, we plan to analyze the evolution of the well-known Greenberger-Horne-Zeilinger (GHZ) state [31]. The results of our calculations reveal that the quantum entanglement for three qubits is more stable than for two qubits. This may be explained by the fact that the three-qubit system is characterized by more degrees of freedom than the two-qubit system. Therefore, based on the reported results of our calculations, one could conclude that the three-qubit system based on excitons in a strained 2D material is a more reliable candidate for quantum technologies than the two-qubitsystem.

ACKNOWLEDGMENTS

O.L.B. is grateful to M. Amico, R. Ya. Kezerashvili, G. V. Kolmakov, and K. G. Ziegler for the valuable discussions. The authors are grateful for support by grants: O.L.B. - the PSC CUNY Grant No. 61538-00 49; O.L.B. and G.P.M. and U.S. ARO grant No. W911NF1810433. GG acknowledges the support from the US AFRL Grant No. FA9453-21-1-0046. The part devoted to new physical realizations of qubits and ququarts was supported by the RFBR grants No. 20- 02-00410 and No. 20-52-00035. Yu.E.L. acknowledged Basic Research Program at the National Research University HSE.

[1] Y. E. Lozovikand A. M. Ruvinsky, Phys. Lett. A **227**, 271 (1997).
[2] Y. E. Lozovikand A. M. Ruvinsky, JETP **85**, 979 (1997).
[3] I. V. Lernerand Y. E. Lozovik, JETP **51**, 588 (1980).
[4] T. Ando, A. B. Fowler, and F. Stern, Rev. Mod. Phys. **54**, 437 (1982).
[5] Y. A. Bychkovand E. I. Rashba, J. Phys. C: Solid state Phys. **17**, 6039 (1984).
[6] C. W. J. Beenakkerand H. van Houten, in *Solid State Physics*, Vol. **44** (Elsevier, 1991) p. 1.
[7] K. S. Novoselov, A. K. Geim, S. V. Morozov, D. Jiang, Y. Zhang, S. V. Dubonos, I. V. Grigorieva, and A. A. Firsov, Science **306**, 666 (2004).
[8] E. McCannand V. I. Fal'ko, Phys. Rev. Lett. **96**, 086805 (2006).
[9] F. Guinea, M. I. Katsnelson, and A. K. Geim, Nature Physics **6**, 30 (2010).
[10] F. Guinea, A. K. Geim, M. I. Katsnelson, and K. S. Novoselov, Phys. Rev. B **81**, 035408 (2010).
[11] M. I. Katsnelson, Materials today **10**, 20 (2007).
[12] B. Amorim, A. Cortijo, F. De Juan, A. G. Grushin, F. Guinea, A. Gutiérrez-Rubio, H. Ochoa, V. Parente, R. Roldán, P. San-Jose, *et al.*, Phys. Rep. **617**, 1 (2016).
[13] F. Guinea, M. I. Katsnelson, and M. A. H. Vozmediano, Phys. Rev. B **77**, 075422 (2008).
[14] N. Levy, S. A. Burke, K. L. Meaker, M. Panlasigui, A. Zettl, F. Guinea, A. H. C. Neto, and M. F. Crommie, Science **329**, 544 (2010).
[15] O. L. Berman, R. Y. Kezerashvili, Y. E. Lozovik, and K. G. Ziegler, Scientific reports **12**, 2950 (2022).
[16] V. Negoita, D. W. Snoke, and K. Eberl, Appl. Phys. Lett. **75**, 2059 (1999).
[17] Z. Vörös, D. W. Snoke, L. Pfeiffer, and K. West, Phys. Rev. Lett. **97**, 016803 (2006).
[18] A. Kormányos, G. Burkard, M. Gmitra, J. Fabian, V. Zólyomi, N. D. Drummond, and V. Fal'ko, 2D Mater. **2**, 022001 (2015).
[19] G. Wang, A. Chernikov, M. M. Glazov, T. F. Heinz, X. Marie, T. Amand, and B. Urbaszek, Rev. Mod. Phys. **90**, 021001 (2018).
[20] E. O. Kiktenko, A. S. Nikolaeva, P. Xu, G. V. Shlyapnikov, and A. K. Fedorov, Phys. Rev. A **101**, 022304 (2020).
[21] B. Roy, V. Juričić, and I. F. Herbut, Phys. Rev. B **87**, 041401(R) (2013)..
[22] H. Shioya, S. Russo, M. Yamamoto, M. F. Craciun, and S. Tarucha, Nano Lett. **15**, 7943 (2015)..
[23] P. Roman-Taboada and G. G. Naumis, Phys. Rev. B **96**, 155435 (2017)..
[24] S. Y. Li, Y. Su, Y. N. Ren, and L. He, Phys. Rev. Lett. **124**, 106802 (2020).
[25] W. K. Wootters, Philosophical Transactions of the Royal Society of London. Series A: Mathematical, Physical and Engineering Sciences **356**, 1717 (1998).
[26] C. H. Bennett, D. P. DiVincenzo, J. A. Smolin, and W. K. Wootters, Phys. Rev. A **54**, 3824 (1996).
[27] V. Vedral, M. B. Plenio, M. A. Rippin, and P. L. Knight, Phys. Rev. Lett. **78**, 2275 (1997).
[28] M. J. Donaldand M. Horodecki, Phys. Lett. A **264**, 257 (1999).
[29] W. K. Wootters, Quantum Inf. Comput. **1**, 27 (2001).

[30] O. L. Berman, R. Y. Kezerashvili, and Y. E. Lozovik, Phys. Rev. A **94**, 052308 (2016).
[31] D. M. Greenberger, M. A. Horne, A. Shimony, and A. Zeilinger, Am. J. Phys. **58**, 1131 (1990).
[32] L. E. Ballentine, *Quantum mechanics: a modern development* (World Scientific, Singapore, 2014).
[33] E. T. Jaynesand F. W. Cummings, Proceedings of the IEEE **51**, 89 (1963).
[34] B. W. Shoreand P. L. Knight, J. Mod. Opt. **40**, 1195 (1993).
[35] M. A. Nielsenand I. Chuang, *Quantum computation and quantum information* (Cambridge University Press, Cambridge, England, 2010).
[36] O. L. Berman, R. Y. Kezerashvili, and Y. E. Lozovik, Phys. Rev. B **80**, 115302 (2009).
[37] K. J. Vahala, Nature **424**, 839 (2003).
[38] D. S. Shapiro, A. A. Zhukov, W. V. Pogosov, and Y. E. Lozovik, Phys. Rev. A **91**, 063814 (2015).
[39] L. S. Bishop, E. Ginossar, and S. M. Girvin, Phys. Rev. Lett. **105**, 100505 (2010).
[40] M. Yönaç, T. Yu, and J. H. Eberly, Journal of Physics B: Atomic, Molecular and Optical Physics **39**, S621 (2006).
[41] I. Sainzand G. Björk, Phys. Rev. A **76**, 042313 (2007).
[42] J. Casanova, G. Romero, I. Lizuain, J. J. García-Ripoll, and E. Solano, Phys. Rev. Lett. **105**, 263603 (2010).

Appendix A: Dissipative dynamics

We determine the solution for the set of differential equations represented by Eq. (32), in the case where only the cavity decay is included ($\gamma = \gamma_\phi - 0$). For this, we first turn our attention to the dissipative term represented by Eq. (33). If $\gamma = \gamma_\phi - 0$, this equation becomes

$$\begin{aligned}\dot{\rho}_{\mathcal{L}_{ij}} &= \langle i| \kappa \mathcal{L}(\hat{a})\rho |j\rangle \\ &= \hat{a}\rho\hat{a}^\dagger - \frac{1}{2}\left(\hat{a}^\dagger\hat{a}\rho + \rho\hat{a}^\dagger\hat{a}\right). \end{aligned} \tag{A1}$$

On this manifold, the effect of the operator $\hat{a}$ is to take the system from the state with one photon and zero excitonic excitations, $|3\rangle = |1;00\rangle$, to the ground state $|0\rangle = |0;00\rangle$, i.e.,

$$\hat{a} = |0\rangle\langle 3| \tag{A2}$$
$$\hat{a}^\dagger = |3\rangle\langle 0|. \tag{A3}$$

Making use of Eq.] (A2-A3) in Eq. (A1), we find

$$\mathcal{L}(\hat{a})\rho = \rho_{33}\left(|0\rangle\langle 0| - |3\rangle\langle 3|\right) - \frac{1}{2}\sum_{j=0}^{2}\left(\rho_{3j}|3\rangle\langle j| + \rho_{j3}|j\rangle\langle 3|\right) , \tag{A4}$$

where $\rho_{ij} = \langle i|\rho|j\rangle$. This leads to

$$\begin{aligned}\dot{\rho}_{\mathcal{L}_{00}} &= \kappa\rho_{33} \\ \dot{\rho}_{\mathcal{L}_{33}} &= -\kappa\rho_{33} \\ \dot{\rho}_{\mathcal{L}_{i3}} &= -\frac{\kappa}{2}\rho_{i3}; i = 0,1,2 \\ \dot{\rho}_{\mathcal{L}_{01}} = \dot{\rho}_{\mathcal{L}_{02}} = \dot{\rho}_{\mathcal{L}_{11}} &= \dot{\rho}_{\mathcal{L}_{12}} = \dot{\rho}_{\mathcal{L}_{22}} = 0 \text{ .}, \end{aligned} \tag{A5}$$

All the other coefficients are obtained by recalling that $\rho_{ij} = \rho^*_{ji}$.

In order to find the terms $\dot{\rho}_{S_{ij}}$, we first determine the result obtained when the Hamiltonian acts on each state of our basis, i.e.,

$$\begin{aligned}\hat{H}|0\rangle &= 0 \\ \hat{H}|1\rangle &= \omega_0|1\rangle + \lambda|3\rangle \\ \hat{H}|2\rangle &= \omega_0|2\rangle + \lambda|3\rangle \\ \hat{H}|3\rangle &= \omega_k|3\rangle + \lambda\left(|1\rangle + |2\rangle\right) . \end{aligned} \tag{A6}$$

Making use of this result in Eq. (30), we find

$$\begin{aligned}
\dot{\rho}_{S_{00}} &= 0 \\
\dot{\rho}_{S_{01}} &= i\omega_0\rho_{01} + i\lambda\rho_{03} \\
\dot{\rho}_{S_{02}} &= i\omega_0\rho_{02} + i\lambda\rho_{03} \\
\dot{\rho}_{S_{03}} &= i\omega_k\rho_{03} + i\lambda(\rho_{01} + \rho_{02}) \\
\dot{\rho}_{S_{11}} &= -i\lambda(\rho_{31} - \rho_{13}) \\
\dot{\rho}_{S_{12}} &= -i\lambda(\rho_{32} - \rho_{13}) \\
\dot{\rho}_{S_{13}} &= -i(\omega_0 - \omega_k)\rho_{13} - i\lambda(\rho_{33} - \rho_{11} - \rho_{12}) \\
\dot{\rho}_{S_{22}} &= -i\lambda(\rho_{32} - \rho_{23}) \\
\dot{\rho}_{S_{23}} &= -i(\omega_0 - \omega_k)\rho_{23} - i\lambda(\rho_{33} - \rho_{22} - \rho_{21}) \\
\dot{\rho}_{S_{33}} &= -i\lambda(\rho_{13} - \rho_{31} + \rho_{23} - \rho_{32}).
\end{aligned} \tag{A7}$$

By combining Eqs. (A5) through (A5), with Eqs. (A7) through (A7) and using the fact that $\rho_{ij} = \rho^*_{ji}$, we can rewrite Eq. (32) as

$$\dot{\rho}_V = \left[i\Lambda + \frac{\kappa}{2}\Gamma\right]\rho_V, \tag{A8}$$

where ρ_V is the column vector

$$\rho_V = (\rho_{00}, \rho_{01}, \rho_{10}, \rho_{02}, \rho_{20}, \rho_{03}, \rho_{30}, \rho_{11}, \rho_{12}, \rho_{21}, \rho_{13}, \rho_{31}, \rho_{22}, \rho_{23}, \rho_{32}, \rho_{33},)^T, \tag{A9}$$

the matrix Λ is given by

$$\Lambda = \begin{pmatrix}
0 & 0 & 0 & 0 & 0 & 0 & 0 & 0 & 0 & 0 & 0 & 0 & 0 & 0 & 0 & 0 \\
0 & \omega_0 & 0 & 0 & 0 & \lambda & 0 & 0 & 0 & 0 & 0 & 0 & 0 & 0 & 0 & 0 \\
0 & 0 & -\omega_0 & 0 & 0 & 0 & -\lambda & 0 & 0 & 0 & 0 & 0 & 0 & 0 & 0 & 0 \\
0 & 0 & 0 & \omega_0 & 0 & \lambda & 0 & 0 & 0 & 0 & 0 & 0 & 0 & 0 & 0 & 0 \\
0 & 0 & 0 & 0 & -\omega_0 & 0 & -\lambda & 0 & 0 & 0 & 0 & 0 & 0 & 0 & 0 & 0 \\
0 & \lambda & 0 & \lambda & 0 & \omega_k & 0 & 0 & 0 & 0 & 0 & 0 & 0 & 0 & 0 & 0 \\
0 & 0 & -\lambda & 0 & -\lambda & 0 & -\omega_k & 0 & 0 & 0 & 0 & 0 & 0 & 0 & 0 & 0 \\
0 & 0 & 0 & 0 & 0 & 0 & 0 & 0 & 0 & 0 & \lambda & -\lambda & 0 & 0 & 0 & 0 \\
0 & 0 & 0 & 0 & 0 & 0 & 0 & 0 & 0 & 0 & \lambda & 0 & 0 & 0 & -\lambda & 0 \\
0 & 0 & 0 & 0 & 0 & 0 & 0 & 0 & 0 & 0 & 0 & -\lambda & 0 & \lambda & 0 & 0 \\
0 & 0 & 0 & 0 & 0 & 0 & 0 & \lambda & \lambda & 0 & (\omega_k - \omega_0) & 0 & 0 & 0 & 0 & -\lambda \\
0 & 0 & 0 & 0 & 0 & 0 & 0 & -\lambda & 0 & -\lambda & 0 & (\omega_0 - \omega_k) & 0 & 0 & 0 & \lambda \\
0 & 0 & 0 & 0 & 0 & 0 & 0 & 0 & 0 & 0 & 0 & 0 & 0 & \lambda & -\lambda & 0 \\
0 & 0 & 0 & 0 & 0 & 0 & 0 & 0 & 0 & \lambda & 0 & 0 & \lambda & (\omega_k - \omega_0) & 0 & -\lambda \\
0 & 0 & 0 & 0 & 0 & 0 & 0 & 0 & -\lambda & 0 & 0 & 0 & -\lambda & 0 & (\omega_0 - \omega_k) & \lambda \\
0 & 0 & 0 & 0 & 0 & 0 & 0 & 0 & 0 & 0 & -\lambda & \lambda & 0 & -\lambda & \lambda & 0
\end{pmatrix}, \tag{A10}$$

and the matrix Γ is given by

$$\Gamma = \begin{pmatrix}
0&0&0&0&0&0&0&0&0&0&0&0&0&0&0&2\\
0&0&0&0&0&0&0&0&0&0&0&0&0&0&0&0\\
0&0&0&0&0&0&0&0&0&0&0&0&0&0&0&0\\
0&0&0&0&0&0&0&0&0&0&0&0&0&0&0&0\\
0&0&0&0&0&0&0&0&0&0&0&0&0&0&0&0\\
0&0&0&0&0&-1&0&0&0&0&0&0&0&0&0&0\\
0&0&0&0&0&0&-1&0&0&0&0&0&0&0&0&0\\
0&0&0&0&0&0&0&0&0&0&0&0&0&0&0&0\\
0&0&0&0&0&0&0&0&0&0&0&0&0&0&0&0\\
0&0&0&0&0&0&0&0&0&0&0&0&0&0&0&0\\
0&0&0&0&0&0&0&0&0&0&-1&0&0&0&0&0\\
0&0&0&0&0&0&0&0&0&0&0&-1&0&0&0&0\\
0&0&0&0&0&0&0&0&0&0&0&0&0&0&0&0\\
0&0&0&0&0&0&0&0&0&0&0&0&0&-1&0&0\\
0&0&0&0&0&0&0&0&0&0&0&0&0&0&-1&0\\
0&0&0&0&0&0&0&0&0&0&0&0&0&0&0&-2
\end{pmatrix}. \tag{A11}$$

First, we note that, as expected, $\dot{\rho}_{00} = -(\dot{\rho}_{11} + \dot{\rho}_{22} + \dot{\rho}_{33})$, which means that the equation for ρ_{00} is redundant and is not needed to solve the system, so we can eliminate the first entry to ρ_V and the first line and column of the matrices Λ and Γ, without any effect. Then, we realize that the remaining problem can be expressed as

$$\dot{\rho}_V = M\rho_V, \tag{A12}$$

where the matrix M can be written as

$$M = \begin{pmatrix} B & 0_{6\times 9} \\ 0_{9\times 6} & A \end{pmatrix}, \tag{A13}$$

where B is a 6×6 matrix, A is a 9×9 matrix and $0_{m\times n}$ is a $m\times n$ matrix with all-zero elements. This means that the time evolution does not mix elements ρ_{0i} with $i\neq 0$ with elements ρ_{ij} with $i,j\neq 0$, nor does it mix ρ_{00} with ρ_{0i} with $i\neq 0$. Therefore, if $|0\rangle\rho\langle i| = 0$ for $i = 1,2,3$ at $t = 0$, $|0\rangle\rho\langle i| = 0$. These are the cases we are interested in, since we want to see how the Hamiltonian eigenvalues $|\psi_0\rangle$ and $|\psi_\pm\rangle$ evolve in time, and they do not involve the state $|0;00\rangle$.

For such cases, the time evolution is given by

$$\dot{\overline{\rho}} = A\overline{\rho} \tag{A14}$$

with

$$\overline{\rho} = (\rho_{11},\rho_{12},\rho_{21},\rho_{13},\rho_{31},\rho_{22},\rho_{23},\rho_{32},\rho_{33})^T \tag{A15}$$

and

$$A = \begin{pmatrix}
0 & 0 & 0 & i\lambda & -i\lambda & 0 & 0 & 0 & 0\\
0 & 0 & 0 & i\lambda & 0 & 0 & 0 & -i\lambda & 0\\
0 & 0 & 0 & 0 & -i\lambda & 0 & i\lambda & 0 & 0\\
i\lambda & i\lambda & 0 & a & 0 & 0 & 0 & 0 & -i\lambda\\
-i\lambda & 0 & -i\lambda & 0 & a^* & 0 & 0 & 0 & i\lambda\\
0 & 0 & 0 & 0 & 0 & 0 & i\lambda & -i\lambda & 0\\
0 & 0 & i\lambda & 0 & 0 & i\lambda & a & 0 & -i\lambda\\
0 & -i\lambda & 0 & 0 & 0 & -i\lambda & 0 & a^* & i\lambda\\
0 & 0 & 0 & -i\lambda & i\lambda & 0 & -i\lambda & i\lambda & -\kappa
\end{pmatrix}, \tag{A16}$$

where $a = -\frac{\kappa}{2} + i(\omega_k - \omega_0)$. Now, all that needs to be done is to find the eigenvectors of this matrix and select from these the ones in which $\rho_{ij} = \rho^*_{ji}$, which will be the ones with meaningful physical reality.

The spectral decomposition of A is rather complicated with very long expressions for most of the eigenvectors and eigenvalues. However, there is one interesting solution that arises with an eigenvalue of zero, which is represented by the vector

$$\overline{\rho}_0 = (1, -1 - 1, 0, 0, 1, 0, 0, 0)^T, \tag{A17}$$

which means that, by going back to the definition of the string $\overline{\rho}$ from Eq. (A15) and using Eq. (42), the state represented by the density operator ρ given by

$$\rho_{ST} = \frac{1}{2}\left(|1\rangle\langle 1| + |2\rangle\langle 2| - |1\rangle\langle 2| - |2\rangle\langle 1|\right) \tag{A18}$$

is a stationary state. It is a simple matter to show that Eq. (A18) canbe expressed as

$$\rho_{ST} = |\Psi^-\rangle\langle\Psi^-| \tag{A19}$$

where the maximum entangled Bell state $|\Psi^-\rangle$ is given by [32]

$$|\Psi^-\rangle = \frac{1}{\sqrt{2}}\left(|1\rangle - |2\rangle\right) = \frac{1}{\sqrt{2}}\left(|0;10\rangle - |0;01\rangle\right). \tag{A20}$$

It is important to note that all other eigenvalues have a negative real part, which means that all other eigenvectors represent states that decay to the ground state exponentially with time. In the case of resonance ($\omega_0 = \omega_k$), the eigenvalues of A are $\lambda_1 = 0$, $\lambda_2 = \lambda_3 = -\frac{\kappa}{2}$, $\lambda_4 = \lambda_5 = -\frac{\kappa}{2} - i\sqrt{32\lambda^2 - \kappa^2}$ and $\lambda_6 = \lambda_7 = \lambda_8 = \lambda_9 = -\frac{\kappa}{4} + i\sqrt{32\lambda^2 - \kappa^2}$, which means that all states other then ρ_{ST} decay with a characteristic time no larger than $\tau = \frac{4}{\kappa}$.